Journal of
Materials Chemistry A

Materials for energy and sustainability

Accepted Manuscript

This article can be cited before page numbers have been issued, to do this please use: S. L. Jain, P. K. Prajapati and S. Saini, *J. Mater. Chem. A*, 2020, DOI: 10.1039/C9TA13801C.

ROYAL SOCIETY OF CHEMISTRY

rsc.li/materials-a

View Article Online
DOI: 10.1039/C9TA13801C

Journal Name

ARTICLE

Nickel mediated Palladium free photocatalytic Suzuki-coupling reaction under visible light irradiation

Received 00th January 20xx,
Accepted 00th January 20xx

DOI: 10.1039/x0xx00000x

www.rsc.org/

Pankaj Kumar Prajapati [a,b] Sandhya Saini [a,b], Suman L. Jain*[a]

The Suzuki coupling is an important, extensively investigated, and manifold approach for C–C bond construction in synthetic chemistry. However, to date, the reaction has been extensively investigated under thermal conditions using palladium-based catalysts. The development of solar light assisted noble-metal free Suzuki coupling represents a green and sustainable approach for such types of reactions. Herein, we describe an efficient, facile, and cost-effective photocatalytic approach for C–C bond formation between aryl halides and phenylboronic acid via Suzuki-cross-coupling using cobalt(II) phthalocyanine complex grafted onto the nickel oxide semiconductor at room temperature (RT) and atmospheric pressure. A number of substituted aryl halides have been successfully investigated under the developed protocol and afforded modest to high yields of the desired biphenyls. The possible mechanistic pathway suggested the formation of photogenerated aryl radical cation from the phenylboronic acid followed by its coupling with aryl radical anion generated from the electron-activated aryl halides resulted in the corresponding biaryls. Importantly, the physical mixture of both components, i.e., CoPc and NiO, showed poor efficiency as compared to the developed hybrid photocatalyst. The recovered photocatalyst could readily be recycled for at least six runs without significant decrease in the activity.

Introduction

Since the discovery in 1979, the palladium-catalyzed Suzuki cross-coupling reaction has proven its versatility and convenient approach for C-C bond construction in the organic synthesis.[1-4] The reactions have been extensively utilized in the preparation of a series of industrially relevant compounds, pharmaceuticals, agrochemicals, and specialty chemicals.[5-7] Generally, activated aryl halides such as substituted bromobenzene and iodobenzene have been effective as substrates due to their high activity.[8] The use of aryl chlorides is a challenging task as the associated Ar–Cl bond possesses high activation barrier, which requires high energy (temperature ≥100 °C) to achieve the formation of targeted C–C bond.[9, 10] A plethora of reports have been published in the prior art mainly using the palladium (Pd) based catalysts, both homogeneous and heterogeneous at high reaction temperatures.[11-14] However, the expensive nature and limited accessibility of the noble metals along with higher energy requirements leave scope for further development of an efficient noble metal-free and less energy-intensive methodology for the Suzuki coupling reaction.[15, 16]

In contrast to the thermal catalytic reactions, photo-induced reactions involve the radical-based mechanistic pathways and occur under ambient conditions in the presence of an inexpensive, renewable and abundantly available solar energy.[17-19] Unlike the thermal catalytic reactions, very few reports are known on the photocatalytic Suzuki reactions. In this context, Li et al. described the coupling between aryl halides and various boronic acids into corresponding biaryls under mild conditions using Mott-Schottky Pd@g-C_3N_4 as a photocatalyst.[20] Wang et al. reported palladium supported on the conjugated microporous polymer as a photocatalyst to afford the biphenyls in bulk.[21] Jiao et al. reported a Mott-Schottky type Pd/SiC heterojunction for coupling of various substituted halobenzenes and phenylboronic acid at 30 °C under visible light irradiation.[22] Sun et al.[23] reported Pd@MOFs catalyzed light assisted coupling of various halobenzenes and aromatic boronic acids at 30 °C to afford excellent yields of biaryls. Chakraborty et al. demonstrated the azobenzene based colloidal porous organic polymer supported Pd-nanoparticle catalysed Suzuki coupling reaction under natural sunlight.[24] Sarina et al.[25] described the enhanced performance of palladium in Pd-Au alloy nanoparticles for copuling of phenyl boronic acid with iodobenzene substrtaes under visible illuminance. Xiao et al.[26] synthesized Pd-Au alloy nanoparticles supported ZrO_2 and studied the coupling between aryl halides

[a] Synthetic Chemistry and Petrochemicals Area, Chemical and Material Sciences Division, CSIR-Indian Institute of Petroleum, Haridwar Road, Mohkampur, Dehradun, India-248005.
[b] Academy of Scientific and Innovative Research (AcSIR), New Delhi, India-110001.
[c] †Electronic Supplementary Information (ESI) available: Technique used, FE-SEM images, EDX pattern, and Elemental mapping of the materials, Gas chromatogram, 1H and 13C NMR spectra of products. See DOI: 10.1039/x0xx00000x

and phenylboronic acid. Mori et al.[27] reported the coupling of a series of substituted bromobenzenes and phenylboronic acid with bimetallic Ru-Pd complex under the visible illumination at room temperature. Gao et al.[28] reported a highly visible light active graphene oxide-Pd functionalized plasmonic Ag-AgBr (GO-Pd@Ag-Br) photocatalyst for biaryls synthesis. Zhang et al.[29] demonstrated the coupling of chemically inert several chlorobenzenes and phenylboronic acid using CeO_2 supported Pd/Au/porous nanorods as a photocatalyst under visible illumination. However, most of the methods are based on the expensive palladium or nable-metal-based catalysts; therefore, it is desired to develop a palladium free, non-noble metal-based green, and sustainable approach for C–C bond construction via Suzuki cross-coupling reactions.

The present paper describes the first report on the use of nickel-based photocatalyst comprising nickel oxide grafted with cobalt(II) phthalocyanine for the photo-induced Suzuki-cross-coupling of phenylboronic acid and a series of chlorobenzenes and bromobenzenes at RT (Scheme 1). The use of low-cost metals (Co, Ni) in the photocatalyst, along with the favourable synergistic effect of both components to afford higher product yields, make this protocol a best-suited and convenient approach for the manufacturing of desired biphenyls under mild operational conditions.

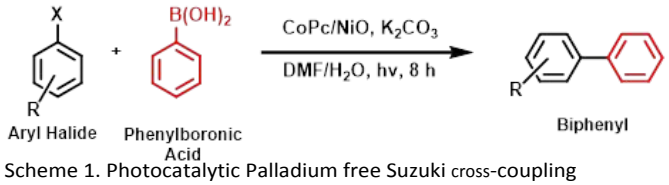

Scheme 1. Photocatalytic Palladium free Suzuki cross-coupling

Results and Discussions

Synthesis and Characterization of the Photocatalyst

The photocatalyst (CNO-10) was synthesized by post-grafting approach using the CoPc (10 wt.%) immobilized to the NiO semiconductor, which was obtained via silica-template assisted protocol as shown in Scheme 2. The cobalt content in CNO-10 photocatalyst was 0.53 wt.%, as determined by ICP-AES.

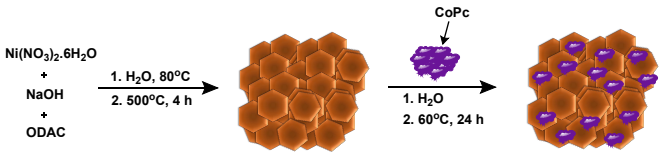

Scheme 2. Synthetic pathways of NiO semiconductor and hybrid CNO-10.

Powder X-ray diffraction determined the crystallinity and lattice-planes in CNO-0 and CNO-10 (Figure 1). NiO shows several sharp diffraction peaks in the diffractogram, which confirms the crystallinity of the material (Figure 1b).[30] The diffraction peaks at 2θ of 37.2°, 43.3°, 62.8°, 75.3°, and 79.4° corresponds to the lattice planes (200), (311), (111), (220) and (222) reveals the presence of nickel in +2 oxidation state in NiO, which also matches well with JCPDS card no. 47-1049 with face-centered cubic lattice.[31] The hybrid CNO-10 exhibits relevant signals at the identical positions in the diffractogram with almost similar intense peaks indicate that the photocatalyst retains the crystallinity after the deposition of the cobalt complex (Figure 1b). Furthermore, the absence of peaks related to the cobalt suggested the minimum deposition of the cobalt complex on NiO surface.

Fig. 1. JCPDS card of a) NiO, Powder diffraction pattern of b) CNO-0,

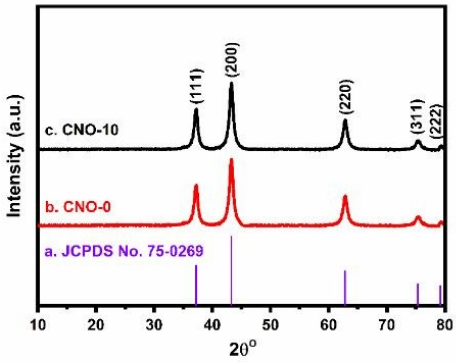

and c) CNO-10 photocatalyst using Cu Kα radiation λ = 0.15418 nm.

FTIR spectral analysis determined the chemical functionalities in the synthesized materials (Figure 2). FTIR spectrum of the cobalt complex shows the characteristic stretching and bending vibrations (Figure 2a).[32] The vibrational peaks between the range 700-1100 cm^{-1} corresponding to the phthalocyanine ring.[33] A moderate vibrational peak at 734 cm^{-1} ascribed the out-of-plane bending for C–H as well as Co–N bonding vibration.[34,35] One more and weak signal at 913 cm^{-1} related to Co–N reveals the bonding of cobalt metal to four surrounding N-atoms of pyrrole rings of phthalocyanine moiety.[36] The stretching vibration at 1164 cm^{-1} and 1521 cm^{-1} are characteristic of the C–H vibration of the aromatic ring and C=C stretching of phthalocyanine ring, respectively.[37] The peak at 1636 cm^{-1} assigned to the C=N stretching vibration and a remote peak at 3434 cm^{-1} represented $–NH_2$ stretching of the pyrrole ring in the complex.[38] FTIR spectrum of NiO semiconductor, revealed two characteristic peaks at 673 cm^{-1} and 1638 cm^{-1} related to the Ni–O–H stretching and H–O–H bending vibrations, respectively (Figure 2b).[39] A broad signal at 1035 cm^{-1} attributed to Si–O–Ni stretching frequency; whereas, the vibrational peak at 1381 cm^{-1} indicated the residual nitrate precursor in NiO semiconductor.[40, 41] A broad peak at 3443 cm^{-1} related to –OH stretching indicated the adsorbed water in the material. After the immobilization, the nanocomposite revealed the characteristic vibrational frequencies of both the components, i.e., cobalt complex and NiO with slight shifting that confirms the successful contact between the complex and the semiconductor (Figure 2c).

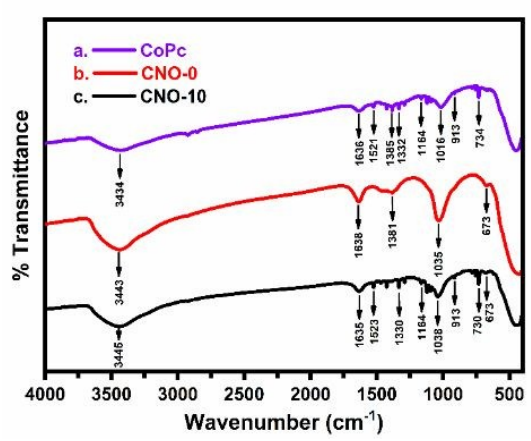

Fig. 2. FTIR spectra of a) CoPc complex, b) CNO-0, and c) CNO-10 photocatalyst.

The absorption spectra of the synthesized materials are represented in figure 3. The cobalt complex shows its characteristic two bands, B-band and Q-band. B-band arises due to $S_0 \rightarrow S_2$ transition in the UV-region ranging from 250-320 nm; Q-band originated due to the metal to ligand charge transfer (MLCT), was appeared in the visible region from 500-720 nm of electromagnetic spectrum (Figure 3a).[42] The HOMO→LUMO transition of π→π* and n→π* splits the Q-band into the two sub-bands, i.e., for aggregated and monomer form of the complex.[43] The absorption spectra of CNO-0 (NiO) mainly absorbed in the UV region ranging from 255-362 nm (Figure 3b).[44] The UV-Vis spectra of hybrid CNO-10, owing to the presence of cobalt complex units, exhibit absorption in the visible region, as depicted in figure 3c. Furthermore, disappearance of the aggregated CoPc absorption band at 560 nm, confirmed the well-dispersed complex units over the NiO support.[45]

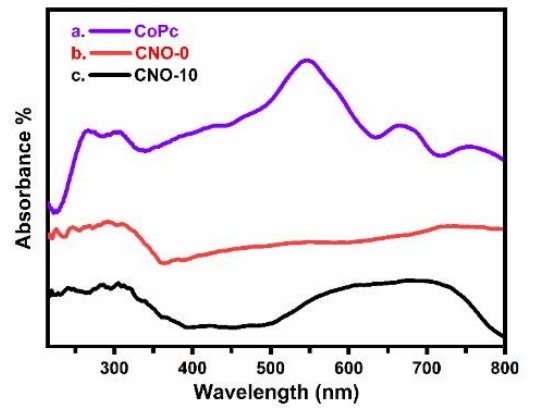

Fig. 3. Ultra-Violet-Visible spectra of a) CoPc complex, b) CNO-0, and c) CNO-10 photocatalyst.

The surface chemical properties of the hybrid determined using X-ray photoelectron spectroscopy (Figure 4). Ni-2p shows a total of six signals in the XPS spectra (Figure 4a). The two XPS peaks at 881.6 eV and 863.0 eV are the satellite peaks, while a 856.0 eV and 857.7 eV represented the Ni-$2p_{3/2}$ and confirm that the nickel presents as Ni^{2+} in the hybrid.[46] The rest two signals at 868.0 eV and 874.4 eV corresponding to Ni-$2p_{1/2}$ of Ni^{2+} oxidation state.[47] Cobalt mainly shows two binding energies for Co-$2p_{3/2}$ and Co-$2p_{1/2}$, where the signal Co-$2p_{3/2}$ splits into the two peaks, at 779.2 eV for octahedral geometry and 781.7 eV for tetrahedral geometry of Co-$2p_{3/2}$, respectively (Figure 4b).[48] The signal at 794.7 eV assigned to Co-$2p_{1/2}$, which confirmed +2 oxidation state of cobalt in the photocatalyst.[49] The XPS spectra of N-1s shows three binding energies; the signal at 401.3 eV and 400.3 eV confirmed the C=N and N–H bonding, respectively of the phthalocyanine moiety, while the third signal at 399.4 eV corresponds to the pyrrolic C–N bonding, representing the metal-ligand interaction (Figure 4c).[50] The presence of all the elements such as Ni-2p, Co-2p, and N-1s, clorresponding to the binding energies 857.9, 781.7, and 400.2 eV, respectively in the survey scan indicated the well-tuned attachment in the hybrid (Figure 4d).

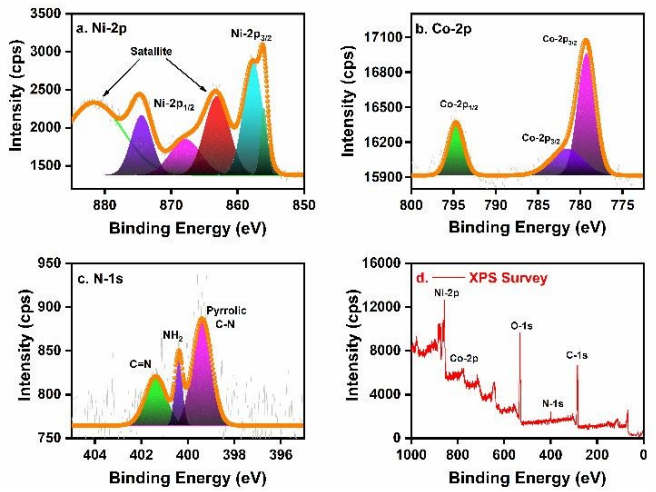

Fig. 4. High-resolution XPS spectra of a) Ni-2p, b) Co-2p, c) N-1s, and d) XPS survey scan for CNO-10 photocatalyst.

The HR-TEM images of as-synthesized semiconductor and hybrid, revealed the surface morphology, microstructure, and the distance between the planes as shown in figure 5. The HR-TEM images show the hexagonal morphology of NiO particles (Figure 5a, b). NiO has a 10 nm particle size, which ascribed at a 10 nm scale (Figure 5a). The interplanar distance of 0.22 nm corresponding to the crystal plane (111), confirms the presence of Ni^{2+} in the semiconductor (Figure 5b). It also matches with the crystal plane at 37.2° in the diffraction pattern. The presence of bright spotted planes in the SAED pattern suggested the crystallinity of NiO semiconductor (Figure 5c). EDX pattern shows the composition of Ni and O-atoms in NiO semiconductor (Figure 5d). Further, the emergence of the dark spots in the hybrid indicated the grafting of CoPc moieties at the surface of NiO semiconductor

View Article Online
DOI: 10.1039/C9TA13801C

(Figure 5e). The distance between the planes of 0.22 nm and 0.25 nm related to (111) and (200) planes, confirmed the presence of Ni^{2+} in the hybrid (Figure 5b & 5f).[31] There was no morphological change observed after the immobilization of the CoPc units, indicating the higher stability of the material. The diffraction planes (111), (200) and (220) revealed in SAED pattern confirm the crystallinity of the hybrid (Figure 5g). The EDX pattern suggested 0.53 wt.% of cobalt content in the hybrid that is in well agreement with the ICP-AES result (Figure 5h). Furthermore, the elemental mapping of NiO and hybrid (CNO-10) suggested the homogeneous dispersion of the cobalt complex throughout the support (Figure S1). The lower deposition of Co-metal particles is further verified by the lower scanned particles in the elemental mapping of the photocatalyst.

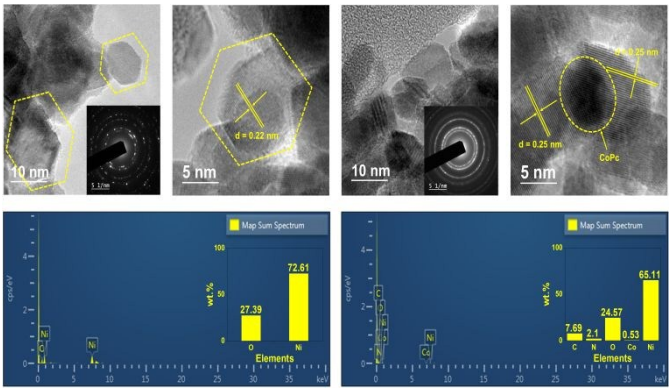

Fig. 5. a) and b) HR-TEM images, c) SAED Pattern, and d) EDX pattern for NiO semiconductor. e) and f) HR-TEM images, g) SAED pattern, and h) EDX pattern of CNO-10 photocatalyst using the lacey carbon grid of mesh size 200.

The electron-hole recombination of photogeneraed charge carriers was determined by photoluminescence (PL) spectroscopy (Figure 6). The PL spectra of bare and CoPc doped NiO excited at 320 nm wavelength at room temperature. The semiconductor CNO-0 of higher crystallinity has a stronger band-band PL emission at 439 nm. Also, the strong band at 439 nm attributed to the surface oxygen vacancies in NiO semiconductor (Figure 6a).[51] The fast recombination of electrons and holes in CNO-0 exhibited an intense PL signal at 439 nm, ascribed the lower charge separation, and more moderate activity under visible illuminance as well. But the high emission indicates the better visible light-emitting ability of NiO nanocrystals at room temperature. The hybrid CNO-10 shows much lower intense, and a broad PL peak at around 435 nm because of blue emission, which originated from the lower recombination of the electron-hole pairs and reveals the higher visible light activity (Figure 6b).[52] The lower intensity of the PL peak in the hybrid due to the deposition of CoPc sensitizer, indicates the smooth transfer of the electrons from LUMO of CoPc to the conduction band of NiO semiconductor (CB) and retarded the electron-hole pair recombination.

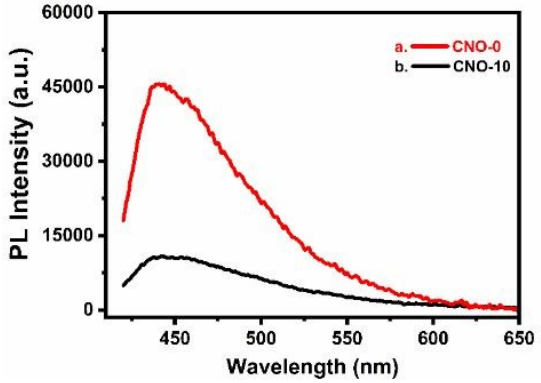

Fig. 6. Photoluminescence spectra of a) CNO-0 semiconductor and b) CNO-10 photocatalyst.

The thermo-gravimetric analysis (TGA) determined the weight loss pattern of the synthesized materials with temperature (Figure 7). The thermogram of CoPc depicts a marginal weight loss up to 200 °C owing to the evaporation of the adsorbed moistures in the complex (Figure 7a). The significant decline in weight occurred at 562 °C attributed to the degradation of the phthalocyanine ring in the complex.[53] The thermogram of NiO shows a minor weight loss below 200 °C due to the absorbed water molecules. After that, the steady line up to 800 °C shows the higher strength of the semiconductor support (Figure 7b).[54] The maximum weight loss obtained for semiconductor was 16%, which exhibits the robust nature of NiO. The hybrid photocatalyst exhibits maximum 20% in between the 450-500 °C attributed the degraded phthalocyanine moieties (Figure 7c).

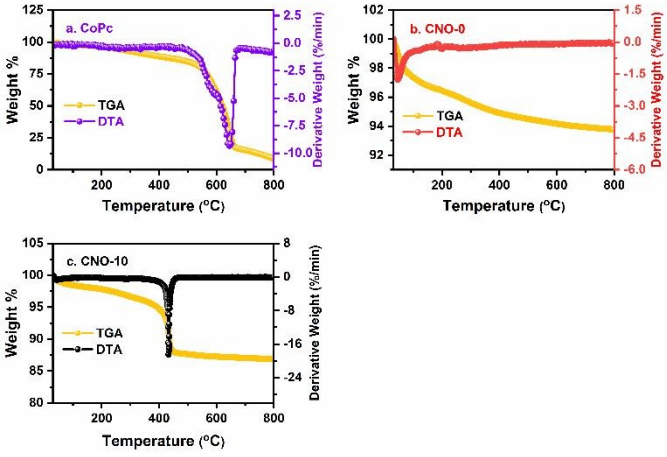

Fig. 7. Thermo-gravimetric analysis of a) CoPc, b) CNO-0, and c) CNO-10 photocatalyst.

The N_2-sorption analysis determined the bulk properties of the synthesized materials using the BET theory (Figure 8). CNO-0 has a high surface area (S_{BET}) of 42.63 m^2/g with the average pore diameter (r_p) of 9.25 nm and pore volume (V_p) of 0.25 cm^3/g. N_2 adsorption-desorption isotherm reveals the type IV isotherm having an H1 hysteresis loop as per the IUPAC classification (Figure 8a).[55] H1 hysteresis loop emerged due to the cylindrical pore distributions in the material. The mean pore diameter of 9.25 nm for CNO-0 lies in the mesoporous range (Figure 8c).[56] The mesoporous nature of CNO-0 semiconductor retains in the hybrid with a slight increase in the BET surface area (45.46 m^2/g) (Figure 8b). The V_p and r_p of the hybrid are found to be 0.192 m^3/g and 4.68 nm, respectively. The isotherm and hysteresis remained almost same in the hybrid; however, a slight decrease in r_p and V_p obtained. The increased surface area of the hybrid photocatalyst attributed to the deposition of CoPc at the exterior of the CNO-0 support; whereas, decreased V_p and r_p values indicates the partial filing of the CoPc units into the pores of the support (Figure 8d).

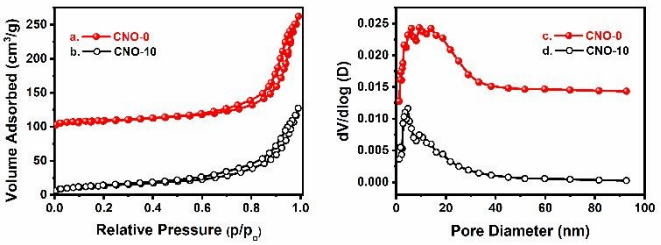

Fig. 8. N_2-sorption isotherm a) & b), and pore size distribution c) & d) of CNO-0 and CNO-10 photocatalyst, respectively analyzed at temperature 77 K.

Photocatalytic Suzuki cross-coupling reaction

The photocatalytic efficiency of the synthesized materials, i.e., CoPc, CNO-0, CNO-5, CNO-10, CNO-15, and CNO-20 was tested for the Suzuki coupling between chlorobenzene and phenylboronic acid at room temperature (27 ℃ ± 2 ℃) under the white LED light having the wavelength (λ) > 400 nm. Table 1 illustrates the results of the optimization studies. The reactivity order of the different hybrid samples having variable amount of CoPc was found to be as CNO-5 < CNO-20 < CNO-15 < CNO-10 (Figure 9). Among all the synthesized materials, CNO-10 exhibited the best activity and provided a maximum 95% conversion with a yield of 92% for the coupling product within 8h (Table 1, entry 6.ii). Further, prolonged the time would not affect the yield of biphenyl. The reduced activity at higher CoPc loading might be due to confined charge mobility resulted from the deposition of the excessive complex molecules on the surface. The reaction did not occur in the dark under otherwise identical conditions. Similarly, there was no reaction observed under visible illumination in the absence of photocatalyst. Subsequently, individual components, e.g., CoPc and CNO-0 remained ineffective under the described conditions. In contrast, the physical mixing of both components in 1:10 ratio by weight (CoPc and NiO) showed slight activity and afforded only 20% yield of the desired product, but most of the CoPc moieties leached out during the reaction (Table 1, entry 7). Among the various solvents studied, a mixed solvent mixture containing DMF/H_2O was found to be optimum (Table 1, entry 6.ii).

Table 1. Suzuki Cross-coupling with different photocatalystsa

S. No.	Solvent	Visible Light	Yield (%)[b]		
			CoPc	CNO-0	CNO-10
1.	DMF/H_2O	No	0	0	0
2.	DMF	Yes	2	< 1	29
3.	H_2O	Yes	2	< 1	23
4.	Toluene	Yes	0	0	16
5.	EtOH/H_2O	Yes	0	0	19
6.i.[c] 6.ii.[d] 6.iii.[e] 6.iv.[f]	DMF/H_2O	Yes	- 11 - -	- 09 - -	47 92 84 69
7.[g]	DMF/H_2O	Yes	-	-	20
8.[h]	DMF/H_2O	Yes	-	-	0

[a]Experimental conditions: chlorobenzene (0.15 mmol), phenylboronic acid (0.165 mmol), K_2CO_3 (2.25 mmol), photocatalyst (30 mg), solvent 4 mL at 27 ± 2 ℃ and atmospheric pressure for 8 h under 20-Watt white LED as a visible light source. [b]Isolated yield. [c]CNO-5. [d]CNO-10. [e]CNO-15. [f]CNO-20. [g]Physically mixed (CoPc+NiO), [h]Without photocatalyst.

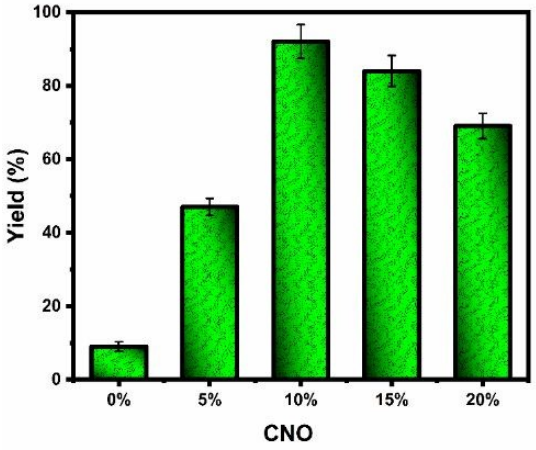

Fig. 9. Effect of variation in the loadings of CoPc on NiO for Suzuki cross-coupling of chlorobenzene and phenylboronic acid.

After the optimization studies, the reaction was generalized with a diverse series of substituted chloro and bromoaryls with phenylboronic acid under the described reaction conditions. The findings of the experiments are summarized in Table 2. All the substrates potentially transformed into the corresponding biphenyls in moderate to high yields using CNO-10 as

photocatalyst in the presence of 1:1 mixture of DMF and H_2O as reaction media under visible light. Among the various substituted substrates, chlorobenzene afforded the highest yield of the coupled product. The presence of electron-withdrawing groups at para-substitution afforded moderate to good yields (Entry 2-4). 1,4-dichlorobenzene, due to the high electronegativity and -I effect of chlorine at para-position of chlorobenzene provided relatively poor yield (83%) of 4-chloro-1,1'-biphenyl (Entry 2). The presence of the highly electron-withdrawing –CN and $–NO_2$ groups at p-position of chlorobenzene reduced the yield of (1,1'-biphenyl)-4-carbonitrile and 4-nitro-1,1'-biphenyl, respectively (Entry 3 & 4). The substitution of -OH group at ortho-position decreased the product yield of (1,1'-biphenyl)-2-ol to 61% (Entry 5), mainly due to the steric hindrance. Similarly, 3,4-dichlorophenol due to the enhanced steric effect afforded poor yield (52%) of the corresponding coupled product (Entry 6). The amino-substituted substrate at para-position afforded slightly higher yield (62%) of (1,1'-biphenyl)-4-amine (Entry 7). 1,2-Dichlorobenzene afforded 66% yield of 2-chloro-1,1'-biphenyl (Entry 8). 3-chloro-*N,N*-dimethylaniline resulted in 68% yield of *N,N*-dimethyl-(1,1'-biphenyl)-3-amine (Entry 9). 4-Chloro-*N,N*-dimethylaniline retained almost similar yield of *N,N*-dimethyl-(1,1'-biphenyl)-4-amine (Entry 10). 4-Methylchlorobenzene with an electron-donating methyl group yielded 59% of 4-methyl-1,1'-biphenyl (Entry 11). The electron-donating methoxy group at para-position resulted in a 71% yield of 4-methoxy-1,1'-biphenyl (Entry 12).

Table 2. Photocatalytic coupling experiments of various chloroarenes and phenylboronic acid under identical conditiona

View Article Online
DOI: 10.1039/C9TA13801C

Sr. No.	Substrate	Product	Conv.[b]	Yield[c]
1.		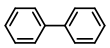	95	92
2.	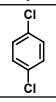	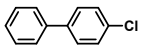	87	83
3.	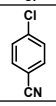	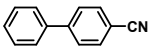	79	77
4.	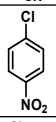	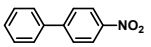	84	81
5.		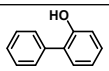	65	61
6.	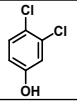	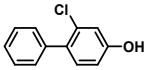	54	52
7.	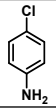	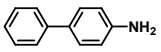	67	62
8.		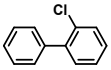	69	66
9.		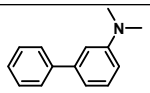	72	68
10.	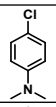	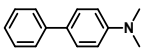	69	66
11.		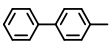	61	59
12.	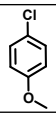	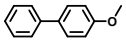	74	71

[a]Experiment: Chloroarene (0.15 mmol), phenylboronic acid (0.165 mmol), K_2CO_3 (2.25 mmol), photocatalyst CNO-10 (30 mg), DMF (2 mL) and H_2O (2 mL) at 27 ± 2 °C and atmospheric pressure for 8 h under 20-Watt white LED as visible light source. [b]Determined by GC-FID. [c]Isolated yield.

View Article Online
DOI: 10.1039/C9TA13801C

The developed protocol also worked efficiently for the cross-coupling reactions between bromobenzenes and phenylboronic acid under identical experimental conditions and gave moderate to high yields of corresponding coupled products (Table 3). Among the various substrates studied, the unsubstituted bromobenzene afforded the highest 78% yield of the biphenyl (Entry 13). In general, the phenyl ring with electron-withdrawing groups (EWG) favored the reaction than electron-donating groups (EDG) and provided a better yield of the desired products.[26] Bromo benzene having $-NO_2$ group at para-position produced an almost similar yield of the corresponding coupled product as the unsubstituted one (Entry 18). Moreover, bromo benzenes having a substitution of the electron-donating group afforded much lower yields of the corresponding biphenyls (Entry 14-17).

Table 3. Photocatalytic coupling of different bromoarenes and phenylboronic acid under identical condition[a]

S. No.	Substrate	Product	Conv.[b]	Yield[c]
13.		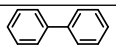	81	78
14.		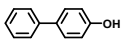	42	39
15.		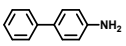	36	31
16.	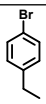	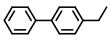	45	43
17.		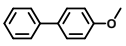	41	36
18.		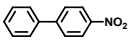	79	77

[a]Experiment: Bromoarene (1.5 mmol), phenylboronic acid (1.65 mmol), K_2CO_3 (2.25 mmol), photocatalyst CNO-10 (30 mg), DMF (2 mL) and H_2O (2 mL) at 27 ± 2 ℃ and atmospheric pressure for 8 h under 20-Watt white LED as visible light source. [b]Determined by GC-FID. [c]Isolated yield.

The recycling experiments performed to evaluate the stability and reusability of the photocatalyst CNO-10. After the coupling reaction of chlorobenzene and phenylboronic acid under optimized conditions, the photocatalyst CNO-10 was isolated from the reaction solution by filtration. The recovered photocatalyst washed with methanol, dried, and used for subsequent runs under identical conditions. As shown in figure 10, the recovered photocatalyst revealed almost consistent activity for at least six cycles. Most importantly, no leaching observed during recycling experiments. After six cycles, the loading of cobalt in the recovered catalyst was 0.51 wt.%, which was almost equivalent to the fresh photocatalyst (0.53 wt.%).

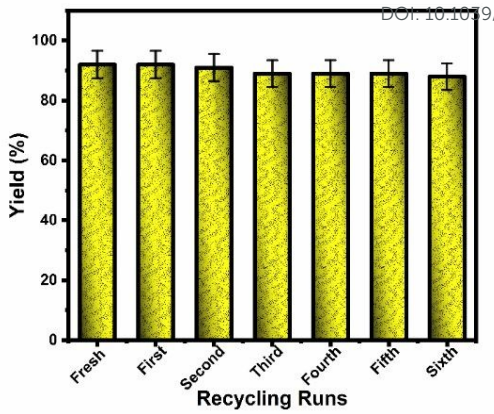

Fig. 10. Recycling runs of the photocatalyst CNO-10 up to six cycles for the Suzuki coupling reaction.

The exact mechanism of the reaction is not known at this stage. Based on the existing reports we elucidated a possible mechanism of the reaction as depicted in Scheme 3. Cobalt phthalocyanine in the hybrid photocatalyst acted as a photosensitizer that ensures the continuous supply of electrons to the conduction band (CB) of the NiO under visible illuminance. Under the light irradiation, CoPc excited and electrons transferred from HOMO to LUMO. Similarly under the light irradiation, the charge separation occurred, and the photogenerated electrons excited from the valance band (VB) to CB of NiO.[57] The photogenerated holes in the HOMO of the CoPc converted the $Ph–\bar{B}(OH)_3$ into the phenyl radical cation. However, the photoexcited electrons in the LUMO of CoPc readily transferred to the conduction band of the NiO and reduced aryl halide to the corresponding aryl anion radical. The holes at the valence band of NiO trapped by the water.[58-60] In a final step the photogenerated phenyl radical cation coupled with radical anion to yield corresponding biphenyl as depicted in Scheme 3.[10,26,61] The attachment of CoPc units on the surface of NiO not only slows down the recombination of the charge carriers, but also reduces the combined band gap of the photocatalyst.[62, 63]

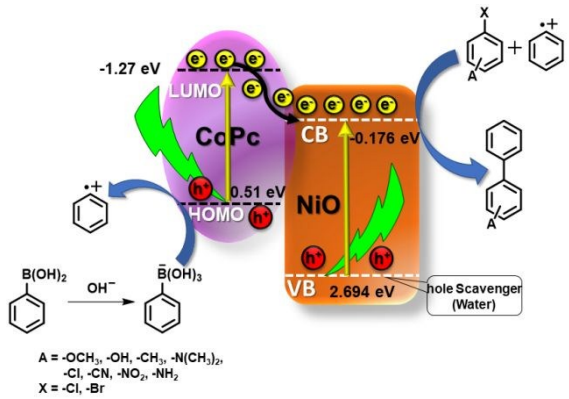

Scheme. 3. Possible mechanism of the photocatalytic Suzuki cross-coupling of haloarenes and phenylboronic acid

Experimental Section

Materials used

The chemicals such as cobalt chloride hexahydrate (Across chemicals), nickel nitrate hexahydrate (Sigma Aldrich), octadecyl dimethyl (3-trimethoxysilylpropyl) ammonium chloride (ODAC) (Sigma Aldrich), hydrazine hydrate (Sigma Aldrich), sodium borohydride (Merck Millipore), sodium hydroxide (Merck Millipore), phthalic anhydride (TCI Chemicals), ammonium molybdate (TCI Chemicals) and urea were purchased and used as received. Cobalt phthalocyanine (CoPc) was synthesized by following the literature reported.[64] All the synthesis and experimental work have been carried out in de-ionized water and absolute ethanol.

Preparation of NiO (CNO-0)

A slightly modified organosilane-template method used to synthesize nickel oxide (NiO) semiconductor.[65] At first, 1.2 g of $Ni(NO_3)_2.6H_2O$ poured into 100 mL of de-ionized water with continuous stirring for 2 h at 40 °C. After the dropwise addition of the 0.6 g ODAC template, the resulted solution warmed up to 60 °C with vigorous stirring for 1 h. The pH maintained at 11.6 by adding the 1 M NaOH to above solution. The solution changed color from green to dark brown, followed by increasing the temperature slowly up to 80 ℃. Vacuum filtration used to separate the precipitates through a membrane filter of 0.45 µm, followed by washing with de-ionized water and dried at 80 °C for whole night. The dried material was heated at 500 °C with 1 ℃/min ramping for 4 h in the presence of air to remove the organosilane-template. Maximum of silica content in the calcined material (1 g) removed by washing with 1M NaOH warmed solution and excess of de-ionized water and ethanol. This material isolated by vacuum filtration and evaporated the moisture content in a vacuum oven at 80 °C for 8 h. The as-prepared NiO semiconductor used further as support for grafting the CoPc complex.

Preparation of CoPc/NiO (CNO) Photocatalyst

CoPc/NiO hybrid was synthesized by following a simple dryness method. In the typical synthesis, 10 mL of NiO (1 g) dispersed de-ionized water sonicated for 1 h, followed by added 10 mL of a certain amount of CoPc (50, 100, 150, and 200 mg) solution with vigorous stirring. The colloidal solution stirred overnight or 24 h for complete evaporation of water content from the sample. The dried sample washed thoroughly with de-ionized water, followed by ethanol to remove excess or unreacted complex moieties. The washed precipitates were heated at 60 °C for 24 h and used for the desired cross-coupling reaction. The different samples containing variable loading of CoPc coded as CNO-5, CNO-10, CNO-15, and CNO-20 for 5%, 10%, 15%, and 20% of CoPc on NiO support, respectively. The best-selected photocatalyst (10%CoPc@NiO) contains 0.53 wt.% of cobalt metal, as ascertained by the ICP-AES technique.

Photocatalytic Coupling Reaction

View Article Online
DOI: 10.1039/C9TA13801C

In the experiment, 1.5 mmol of haloarene, 1.65 mmol of phenylboronic acid, 2.25 mmol of potassium carbonate, and 4 mL of DMF/H_2O in 1:1 ratio poured into a 50 mL round bottom (RB) flask. The flask closed tightly with a septum followed by a flow of N_2 gas for 10 min to create an inert environment in the vessel with continuous stirring. After that, RB charged with 30 mg of CNO-10 photocatalyst, and the RB was irradiated under the 20 Watt LED as a white light source. TLC analyzed the reaction progress after every 1 h interval. The maximum conversion of the aryl halides under the developed protocol observed in 8 h; therefore, it is considered as the optimum reaction time. After 8 h of the experiment, the resulting mixture was withdrawn using a syringe and filtered through the Millipore filter (0.45 µm) to remove the photocatalyst. The product was extracted with ethyl acetate and *n*-hexane in 9: 1 ratio through microcolumn fitted with the silica-gel. GC-FID determined the conversion and yield of the coupling products to quantify the reaction products. ^1H & ^{13}C NMR confirmed the products by comparing the spectral data of the authentic compounds.

Conclusions

The present paper demonstrated the first successful palladium free visible light assisted Suzuki-cross-coupling reaction between various haloarenes and phenylboronic acid using cobalt phthalocyanine grafted NiO (CNO) photocatalyst at room temperature. The developed protocol worked efficiently for a vast range of substituted chloro and bromobenzenes to yield the corresponding coupled product in moderate to excellent yields. Under the developed protocol, the maximum 95% conversion of chlorobenzene with a yield of 92% of biphenyl was achieved. Under similar experimental conditions, the bare CoPc and NiO did not show any efficiency, whereas a physical mixture of both components showed a significantly reduced activity. The CoPc acted as a photosensitizer that provided a continuous supply of electrons to the CB of the semiconductor. The presence of the base also played a vital role and facilitated the formation of the quaternary boronic acid anion. The developed photocatalyst could easily be separated and successfully recycled after several runs with almost consistent efficiency. The present work demonstrates a sustainable approach for the formation of C-C bonds by using a cost-effective nickel-based photocatalyst under palladium free conditions with the added benefits of using abundantly available solar energy under ambient temperature compounds.

Acknowledgements

The authors kindly acknowledge, Director CSIR-IIP for his permission to publish these results. PKP and SS acknowledge CSIR-New Delhi, India, for their research fellowships. This work was funded by SERB-DST in the form of a project GAP-3125. AcSIR-New Delhi, India, is highly acknowledged for the

registration of Ph.D. Authors are grateful to the Analytical Section Division for providing analysis of the samples.

ORCID

Suman L. Jain: 0000-0002-4198-040X

Pankaj Kumar Prajapati: 0000-0001-7012-1017

Conflicts of interest

The authors declare no conflict of interest.

Notes and references

1. E. Negishi, *Acc. Chem. Res.*, 1982, **15**, 340-348.
2. Y. Tamaki, T. Morimoto, K. Koike and O. Ishitani, *Proc. Natl. Acad. Sci. U.S.A.*, 2012, **109**, 15673-15678.
3. N. Miyaura and S. L. Buchwald, *Cross-coupling reactions: a practical guide*, Springer, 2002.
4. A. Suzuki, *J. Organomet. Chem.*, 2002, **653**, 83-90.
5. C. Torborg and M. Beller, *Adv. Synth. Catal.*, 2009, **351**, 3027-3043.
6. P. Devendar, R.-Y. Qu, W.-M. Kang, B. He and G.-F. Yang, *J. Agric. Food. Chem.*, 2018, **66**, 8914-8934.
7. J. H. Clark, *J. Chem. Technol. Biotechnol.*, 2007, **82**, 603-609.
8. M. Durandetti, J.-Y. Nédélec and J. Périchon, *J. Org. Chem.*, 1996, **61**, 1748-1755.
9. N. E. Leadbeater and M. Marco, *J. Org. Chem.*, 2003, **68**, 888-892.
10. M. B. Thathagar, J. Beckers and G. Rothenberg, *J. Am. Chem. Soc.*, 2002, **124**, 11858-11859.
11. R. Martin and S. L. Buchwald, *Acc. Chem. Res.*, 2008, **41**, 1461-1473.
12. S.-Y. Ding, J. Gao, Q. Wang, Y. Zhang, W.-G. Song, C.-Y. Su and W. Wang, *J. Am. Chem. Soc.*, 2011, **133**, 19816-19822.
13. G. C. Fortman and S. P. Nolan, *Chem. Soc. Rev.*, 2011, **40**, 5151-5169.
14. C. R. LeBlond, A. T. Andrews, Y. Sun and J. R. Sowa, *Org. Lett.*, 2001, **3**, 1555-1557.
15. G. Zhang, Y. Peng, L. Cui and L. Zhang, *Angew. Chem. Int. Ed.*, 2009, **48**, 3112-3115.
16. D. Astruc, *Inorg. Chem.*, 2007, **46**, 1884-1894.
17. Z. Wang, W. Mao, H. Chen, F. Zhang, X. Fan and G. Qian, *Catal. Commun.*, 2006, **7**, 518-522.
18. N. S. J. s. Lewis, *Science*, 2007, **315**, 798-801.
19. Z.-R. Tang, Y. Zhang and Y.-J. Xu, *ACS Appl. Mater. Interfaces*, 2012, **4**, 1512-1520.
20. X.-H. Li, M. Baar, S. Blechert and M. Antonietti, *Sci. Rep.*, 2013, **3**, 1743.
21. Z. J. Wang, S. Ghasimi, K. Landfester and K. A. Zhang, *Chem. Mater.*, 2015, **27**, 1921-1924.
22. Z. Jiao, Z. Zhai, X. Guo and X.-Y. Guo, *J. Phys. Chem. C*, 2015, **119**, 3238-3243.
23. D. Sun and Z. Li, *J. Phys. Chem. C*, 2016, **120**, 19744-19750.
24. J. Chakraborty, I. Nath and F. Verpoort, *Chem. Eng. J.*, 2019, **358**, 580-588.
25. S. Sarina, H. Zhu, E. Jaatinen, Q. Xiao, H. Liu, J. Jia, C. Chen and J. Zhao, *J. Am. Chem. Soc.*, 2013, **135**, 5793-5801.
26. Q. Xiao, S. Sarina, E. Jaatinen, J. Jia, D. P. Arnold, H. Liu and H. Zhu, *Green Chem.*, 2014, **16**, 4272-4285.
27. K. Mori, M. Kawashima and H. Yamashita, *Chem. Commun.*, 2014, **50**, 14501-14503.
28. S. Gao, N. Shang, C. Feng, C. Wang and Z. Wang, *RSC Adv.*, 2014, **4**, 39242-39247.
29. S. Zhang, C. Chang, Z. Huang, Y. Ma, W. Gao, J. Li and Y. Qu, *ACS Catal.*, 2015, **5**, 6481-6488.
30. S. P. Patil, L. Jadhav, D. P. Dubal and V. Puri, *Mater. Sci. Poland*, 2016, **34**, 266-274.
31. N. Srivastava and P. Srivastava, *Bull. Mater. Sci.*, 2010, **33**, 653-656.
32. L. Zhu, X. Jing, L. Song, B. Liu, Y. Zhou, Y. Xiang and D. Xia, *New J. Chem.*, 2014, **38**, 663-668.
33. R. Seoudi, G. El-Bahy and Z. El Sayed, *J. Mol. Struct.*, 2005, **753**, 119-126.
34. A. Sidorov, *Opt. Spectrosc.*, 1976, **40**, 280-283.
35. G. Meshkova, A. Vartanyan and A. N. Sidorov, *Opt. Spectrosc.*, 1977, **43**, 151-154.
36. T. Kobayashi, F. Kurokawa, N. Uyeda and E. Suito, *Spectrochim. Acta Part A*, 1970, **26**, 1305-1311.
37. G. Liu, S. Liu, Q. Lu, H. Sun and Z. Xiu, *RSC Adv.*, 2014, **4**, 53402-53406.
38. A. Kumar, P. K. Prajapati, M. Aathira, A. Bansiwal, R. Boukherroub and S. L. Jain, *J. Colloid Interface Sci.*, 2019, **543**, 201-213.
39. F. Thema, E. Manikandan, A. Gurib-Fakim and M. Maaza, *J. Alloys Compd.*, 2016, **657**, 655-661.
40. C. Lei, X. Zhu, B. Zhu, J. Yu and W. Ho, *J. Colloid Interface Sci.*, 2016, **466**, 238-246.
41. W. A. W. A. Bakar, R. Ali and N. S. Mohammad, *Arab. J. Chem.*, 2015, **8**, 632-643.
42. M. Gouterman, *J. Mol. Spectrosc.*, 1961, **6**, 138-163.
43. P. K. Prajapati, A. Kumar and S. L. Jain, *ACS Sustain. Chem. Eng.*, 2018, **6**, 7799-7809.
44. T. Shahid, T. Khan, M. Zakria, R. Shakoor and M. Arfan, *J Mater Sci and Eng*, 2016, **5**, 6.
45. P. K. Prajapati and S. L. Jain, *Dalton Trans.*, 2019, **48**, 4941-4948.
46. M. A. Peck and M. A. Langell, *Chem. Mater.*, 2012, **24**, 4483-4490.
47. C. Guan, Y. Wang, Y. Hu, J. Liu, K. H. Ho, W. Zhao, Z. Fan, Z. Shen, H. Zhang and J. Wang, *J. Mater. Chem. A*, 2015, **3**, 23283-23288.
48. Z. Zhou, Y. Zhang, Z. Wang, W. Wei, W. Tang, J. Shi and R. Xiong, *Appl. Surf. Sci.*, 2008, **254**, 6972-6975.
49. T. Zhang, X. Wang, X. Huang, Y. Liao and J. Chen, *RSC Adv.*, 2016, **6**, 2810-2818.
50. P. Kumar, A. Kumar, B. Sreedhar, B. Sain, S. S. Ray and S. L. Jain, *Chem. Eur. J.*, 2014, **20**, 6154-6161.
51. M. Zhou, J. Yu, S. Liu, P. Zhai and L. Jiang, *J. Hazard. Mater.*, 2008, **154**, 1141-1148.
52. S. M. Meybodi, S. Hosseini, M. Rezaee, S. Sadrnezhaad and D. Mohammadyani, *Ultrason. Sonochem.*, 2012, **19**, 841-845.
53. P. Kumar, A. Kumar, C. Joshi, R. Singh, S. Saran and S. L. Jain, *RSC Adv.*, 2015, **5**, 42414-42421.
54. M. B. Mahajan and P. A. Joy, *Phys. Chem. Chem. Phys.*, 2013, **15**, 20808-20812.
55. S. Saini, H. Singh, P. K. Prajapati, A. K. Sinha and S. L. Jain, *ACS Sustain. Chem. Eng.*, 2019, **7**, 11313-11322.

View Article Online
DOI: 10.1039/C9TA13801C

56. T. Alammar, O. Shekhah, J. Wohlgemuth and A.-V. Mudring, *J. Mater. Chem.*, 2012, **22**, 18252-18260.
57. M. Zanjanchi, A. Ebrahimian and M. Arvand, *J. Hazard. Mater.*, 2010, **175**, 992-1000.
58. K. Doudrick, T. Yang, K. Hristovski and P. Westerhoff, *Appl. Catal. B*, 2013, **136**, 40-47.
59. F. Raza, D. Yim, J. H. Park, H.-I. Kim, S.-J. Jeon and J.-H. Kim, *J. Am. Chem. Soc.*, 2017, **139**, 14767-14774.
60. D. Yim, F. Raza, J. H. Park, J.-H. Lee, H.-I. Kim, J.-K. Yang, I.-J. Hwang and J.-H. Kim, *ACS Appl. Mater. Interfaces*, 2019, **11**, 36960-36969.
61. S. MacQuarrie, J. H. Horton, J. Barnes, K. McEleney, H. P. Loock and C. M. Crudden, *Angew. Chem. Int. Ed.*, 2008, **47**, 3279-3282.
62. G. M. Neelgund, A. Oki and Z. Luo, *J. Colloid Interface Sci.*, 2014, **430**, 257-264.
63. R. Salinas-Guzman, J. Guzmán-Mar, L. Hinojosa-Reyes, J. Peralta-Hernández and A. Hernandez-Ramirez, *J. Sol-Gel Sci. Technol.*, 2010, **54**, 1-7.
64. M. Mahyari and A. Shaabani, *Appl. Catal., A*, 2014, **469**, 524-531.
65. P. K. Prajapati, H. Singh, R. Yadav, A. K. Sinha, S. Szunerits, R. Boukherroub and S. L. Jain, *Appl. Surf. Sci.*, 2019, **467**, 370-381.